Biochimica et Biophysica Acta 1840 (2014) 332–343

Contents lists available at ScienceDirect

Biochimica et Biophysica Acta

journal homepage: www.elsevier.com/locate/bbagen

Design and discovery of novel quinazolinedione-based redox modulators as therapies for pancreatic cancer

Divya Pathania [a], Mario Sechi [b,*], Michele Palomba [b], Vanna Sanna [b], Francesco Berrettini [c], Angela Sias [b], Laleh Taheri [a], Nouri Neamati [a,**,1]

[a] Department of Pharmacology and Pharmaceutical Sciences, University of Southern California, School of Pharmacy, 1985 Zonal Avenue, Los Angeles, CA, USA
[b] Dipartimento di Chimica e Farmacia, Università di Sassari, Via Vienna 2, 07100 Sassari, Italy
[c] Centro Analisi e Determinazioni Strutturali, Università di Siena, Via Aldo Moro 2, 53100 Siena, Italy

ARTICLE INFO

Article history:
Received 22 March 2013
Received in revised form 23 July 2013
Accepted 8 August 2013
Available online 15 August 2013

Keywords:
Redox regulation
Small molecule drug discovery
Anticancer compounds
Oxidative stress in cancer cells
ROS-mediated cell death

ABSTRACT

Background: Altered cellular bioenergetics and oxidative stress are emerging hallmarks of most cancers including pancreatic cancer. Elevated levels of intrinsic reactive oxygen species (ROS) in tumors make them more susceptible to exogenously induced oxidative stress. Excessive oxidative insults overwhelm their adaptive antioxidant capacity and trigger ROS-mediated cell death. Recently, we have discovered a novel class of quinazolinediones that exert their cytotoxic effects by modulating ROS-mediated signaling.

Methods: Cytotoxic potential was determined by colorimetric and colony formation assays. An XF24 Extracellular Flux Analyzer, and colorimetric and fluorescent techniques were used to assess the bioenergetics and oxidative stress effects, respectively. Mechanism was determined by Western blots.

Results: Compound **3a** (6-[(2-acetylphenyl)amino]quinazoline-5,8-dione) was identified through a medium throughput screen of ~1000 highly diverse in-house compounds and chemotherapeutic agents for their ability to alter cellular bioenergetics. Further structural optimizations led to the discovery of a more potent analog, **3b** (6-[(3-acetylphenyl)amino]quinazoline-5,8-dione) that displayed anti-proliferative activities in low micromolar range in both drug-sensitive and drug-resistant cancer cells. Treatment with **3b** causes Akt activation resulting in increased cellular oxygen consumption and oxidative stress in pancreatic cancer cells. Moreover, oxidative stress induced by **3b** promoted activation of stress kinases (p38/JNK) resulting in cancer cell death. Treatment with antioxidants was able to reduce cell death confirming ROS-mediated cytotoxicity.

Conclusion: In conclusion, our novel quinazolinediones are promising lead compounds that selectively induce ROS-mediated cell death in cancer cells and warrant further preclinical studies.

General significance: Since **3b** (6-[(3-acetylphenyl)amino]quinazoline-5,8-dione) exerts Akt-dependent ROS-mediated cell death, it might provide potential therapeutic options for chemoresistant and Akt-overexpressing cancers.

1. Introduction

Pancreatic cancer is a multifaceted disorder with poor prognosis. The five-year survival rate is only 5.6% [1]. The major obstacles in the successful treatment of pancreatic cancer are its inherent high resistance to existing chemotherapy and its late-stage detection. Therefore, there is an urgent need to develop new and safe drugs for effective treatment of late stage and resistant pancreatic cancer. A new strategy is to target emerging hallmarks of cancer cells such as metabolic reprogramming and oxidative stress [2]. Aerobic glycolysis, glutamine dependent anaplerosis, de novo lipid and nucleotide biosynthesis and oxidative stress are some of the key bioenergetic alterations observed in cancer cells [3].

Oxidative stress is an important hallmark of most cancer cells including pancreatic cancer [4]. Reactive oxygen species (ROS) including free radicals (superoxide anion, hydroxyl radical) and non-radical species (hydrogen peroxide) are highly reactive and can be detrimental

Abbreviations: CMFDA, 5-chloromethylfluorescein diacetate; DMEM, Dulbecco's Modified Eagle Medium; DMSO, dimethyl sulfoxide; DNA, deoxyribonucleic acid; DPBS, Dulbecco's Phosphate Buffered Saline; DRAQ5®, 1,5-bis{[2-(di-methylamino) ethyl] amino}-4,8-dihydroxyanthracene-9,10-dione; EDTA, ethylene diaminetetraacetic acid; FoxO3a, forkhead box transcription factor 3a; GAPDH, glyceraldehyde 3-phosphate dehydrogenase; GSH, glutathione (reduced); JNK, c-Jun N-terminal kinase; MnSOD, manganese superoxide dismutase, MTT, 3-(4,5-dimethylthiazol-2-yl)-2,5-diphenyltetrazolium bromide; NAC, *N*-acetylcysteine; NADPH, nicotinamide adenine dinucleotide phosphate (reduced); NO-ASA, 3-Nitrooxyphenyl acetylsalicylate; NOX1, NADPH oxidase; NQO1, NAD(P)H dehydrogenase (quinone) 1; OCR, oxygen consumption rate; RIPA buffer, Radio-Immunoprecipitation Assay buffer; ROS, reactive oxygen species; RPMI-1640, Roswell Park Memorial Institute-1640

* Corresponding author. Tel.: +39 079 228 753; fax: +39 079 229 559.
** Correspondence to: N. Neamati, Department of Pharmacology and Pharmaceutical Sciences, University of Southern California, School of Pharmacy, 1985 Zonal Avenue, PSC 304, Los Angeles, CA 90089, USA. Tel.: +1 323 442 2341; fax: +1 323 442 1390.
E-mail addresses: mario.sechi@uniss.it (M. Sechi), neamati@usc.edu, neamati@umich.edu (N. Neamati).
[1] New Address: Nouri Neamati, Ph.D., Department of Medicinal Chemistry, College of Pharmacy, University of Michigan, North Campus Research Complex, 2800 Plymouth Road, Bldg 520, Room 1363, Ann Arbor, MI 48109-2800, USA. Tel.: +1 734 647 2732; fax: +1 734 647 8430.

0304-4165/$ – see front matter © 2013 Elsevier B.V. All rights reserved.
http://dx.doi.org/10.1016/j.bbagen.2013.08.005

when present at a high concentration. Cells maintain a state of redox homeostasis by regulating the equilibrium between ROS generation and scavenging. ROS are generated in biological systems by various enzymatic (i.e. NADPH oxidase) and non-enzymatic (mitochondrial electron transport chain) processes. To maintain ROS below their detrimental levels, several antioxidant enzymes such as superoxide dismutase, glutathione peroxidase, peroxiredoxins, glutaredoxin, thioredoxin and catalase act as ROS scavengers [5].

ROS play an important role as second messengers in cell signaling and regulate a myriad of signal transduction pathways and cell cycle events [6,7]. ROS have also been implicated in various diseases including cancer, neurodegenerative diseases, diabetes, cardiac disorders and mitochondrial diseases. Therefore, maintaining a balance between ROS generation and degradation is essential for normal cell proliferation, growth and survival [8]. Increased synthesis and/or decreased elimination of ROS result in oxidative stress leading to deleterious effects on cellular proteins, lipids and nucleic acids. Moreover, ROS regulate several processes associated with cancer development and tumor invasiveness [9,10]. Increased ROS levels are known to facilitate tumor initiation and progression [11] by inducing DNA damage leading to oncogenic transformation [12]. Therefore, several therapeutic strategies focus on the use of antioxidants as cancer preventive agents [13].

In addition to their tumor promoting actions, ROS exert a critical effect on cell migration by activating specific genes to promote epithelial–mesenchymal like transition and metastasis. Furthermore, cancer cells are known to develop adaptive responses to increased ROS levels to cope with the hazardous effects of oxidative stress [14,15]. These include the activation of redox sensitive transcription factors that increase the expression of endogenous antioxidants, promote survival pathways, induce chemoresistance and alter caspase activation [16,17]. Despite this adaptive mechanism, higher basal ROS levels make cancer cells more susceptible to exogenously induced ROS-mediated cell death. Excessive supply of exogenous oxidative insults will overwhelm the adaptive capacity of cancer cells and promote cell death [16]. Increasing ROS production or decreasing ROS scavenging has shown a therapeutic potential for selectively targeting tumor cells that are under persistent oxidative stress (Fig. 1). This suggests a "two-faced" or dual role of ROS in cancer [18,19]. At lower levels they act as tumor promoters, whereas in excessive amount they cause cell death. Furthermore, ROS-mediated anticancer therapy aids in overcoming resistance associated with other antineoplastic agents [20].

Developing compounds that exploit the high basal ROS levels uniquely present in cancer cells is an innovative and promising approach in drug discovery [16]. ROS inducers, agents decreasing cellular oxidative-buffering capacity, or a combination of both, can produce exogenous oxidative stress. Normal cells have much lower ROS levels as compared to cancer cells, and enjoy a higher antioxidant and oxidative-buffering reserve to deal with exogenous ROS insults. Therefore, it has been shown that these agents are not significantly toxic to normal cells [21].

Since increased bioenergetic alterations and oxidative stress are hallmarks of most forms of cancer, we were interested in discovering compounds that influence cancer cell bioenergetics. The novel compounds described herein targeting the altered cellular bioenergetic characteristic of cancer cells, were identified in a medium throughput screen using an XF24 Extracellular Flux Analyzer (Seahorse Bioscience, Billerica, MD). XF24 measures the rates of cellular oxygen consumption and extracellular acidification in real time. Cancer cells were exposed to a library of small molecule compounds including novel anticancer agents in our laboratory, known chemotherapeutic agents and novel small molecule compounds designed by us. The screen was performed for finding agents that would alter cellular bioenergetics in cancer cells. Through our screening we identified two classes of potential anticancer agents, triphenylphosphoniums [22] and quinazoline-5,8-diones (**3a**-**f**,**4**) (Table 1). Triphenylphosphoniums decreased cellular oxygen consumption rate (OCR) whereas our novel quinazoline-5,8-diones resulted in tremendous increase in cellular OCR. Our novel small molecule quinazoline-5,8-diones exert the highest level of reported increase in cellular oxygen consumption rate in cancer cells resulting in ROS production and exogenous oxidative stress. The incremental ROS generation induced by these compounds in combination with the higher ROS level present in cancer cells leads to the activation of stress related MAP kinases (p38 and JNK) culminating in cell death.

2. Materials and methods

2.1. Cell culture

Pancreatic cancer (MIA PaCa-2, PANC-1 and BxPC-3), breast cancer (T-47D, MDA-MB-231, MDA-MB-435 and MCF7), lung cancer (NCI-H460 and NCI-H1299), and prostate cancer (PC-3) cell lines were purchased from the American Type Cell Culture (Manassas, VA). HCT116 $p53^{+/+}$ and HCT116 $p53^{-/-}$ cells were kindly provided by Dr. Bert Vogelstein (The Sidney Kimmel Comprehensive Cancer Center, Baltimore, MD). Human ovarian carcinoma cell line (HEY) naturally resistant to cisplatin (CDDP) was kindly provided by Dr. Louis Dubeau (USC Norris Cancer Center, Los Angeles, CA) [23,24]. OVCAR-8 (ovarian cancer) and multi-drug resistant NCI/ADR-RES cells were obtained from the Developmental Therapeutics Program, NCI (Bethesda, MD). Dr. Carla Grandori (Fred Hutchinson Cancer Research Center, Seattle, WA) kindly provided

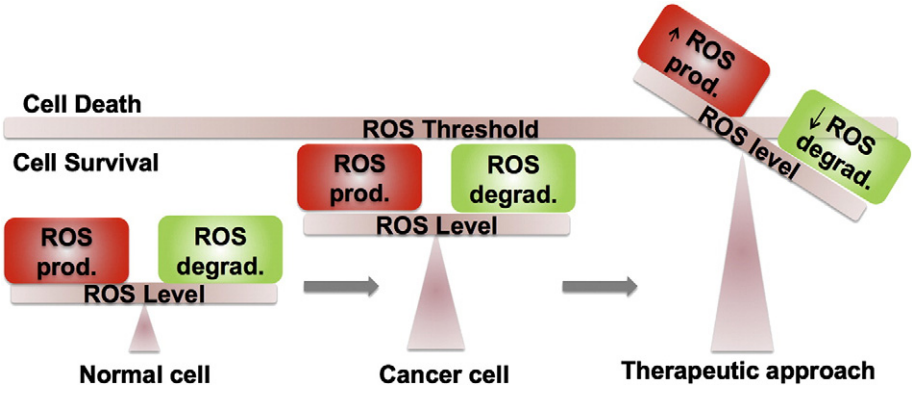

Fig. 1. Rationale for ROS-mediated cancer therapy. Normal cells regulate cellular redox homeostasis by maintaining a balance between ROS generation and scavenging. Oxidative stress is a characteristic of most forms of cancer. Increased ROS levels promote tumor initiation, progression and metastasis. Cancer cells are known to develop adaptive responses to increased ROS levels to protect themselves from the hazardous effects of oxidative stress. However, higher basal ROS levels make cancer cells more susceptible to exogenously induced ROS-mediated cell death. Excessive supply of exogenous oxidative insults will overwhelm the adaptive capacity of cancer cells, promote cell death and can be exploited as a therapeutic approach. (prod., production; degrad., degradation).

Table 1
Cytotoxicity of compounds **3a–f**, and **4** in pancreatic cancer cell lines.

		IC_{50} (μM)[a]		
Compound	Structure	BxPC-3	MIA PaCa-2	PANC-1
3a	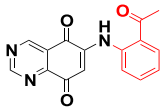	2.7 ± 0.3	1.9 ± 0.1	2.2 ± 0.3
3b	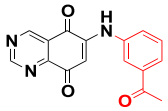	2.4 ± 0.1	2.3 ± 0.2	2.0 ± 0.2
3c	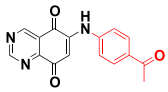	2.2 ± 0.2	1.7 ± 0.4	1.9 ± 0.3
3d	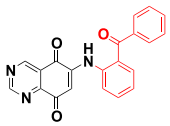	6.5 ± 0.1	3.4 ± 0.2	4.1 ± 0.8
3e	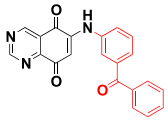	3.1 ± 0.9	3.1 ± 0.4	2.1 ± 0.4
3f	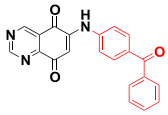	7.8 ± 0.3	1.6 ± 0.2	1.8 ± 0.3
4	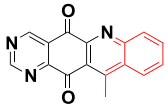	2.0 ± 0.0	2.3 ± 0.5	2.3 ± 0.5
Gemcitabine	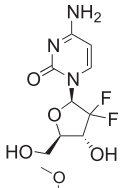	0.026 ± 0.003	0.042 ± 0.018	2.8 ± 1.7
Erlotinib	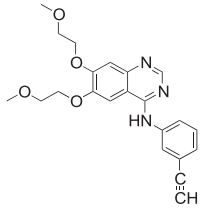	>10	>10	>10
Resveratrol	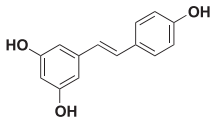	>10	>10	>10
Sodium lipoate (lipoic acid)	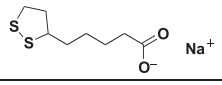	>10	>10	>10

[a] IC_{50} is defined as drug concentration causing a 50% decrease in cell population using MTT assay. Values with standard deviation are from at least three independent experiments. Each experiment was generated from an average of three independent wells. The concentrations of DMSO used in the experiments were not cytotoxic to cells.

the human foreskin fibroblast cell lines (HFF-1) [25]. All cell lines used for experiments were maintained in culture under 35 (15 for HFF-1) passages and tested regularly for *mycoplasma* contamination using Plasmo Test™ (InvivoGen, San Diego, CA). Cell lines were maintained in the appropriate growth media (DMEM [Cellgro, Mediatech, Mannassas, VA] for MDA-MB-435, MDA-MB-231, MCF7, PANC-1, MIA PaCa-2, PC-3; RPMI-1640 [(Cellgro, Mediatech, Mannassas, VA] for BxPC-3, HEY, NCI/ADR-RES, NCI-H1299, NCI-H460, T47-D, OVCAR-8, HFF-1 and HCT116 cell lines) containing 10% heat-inactivated fetal bovine serum (Gemini-Bioproducts, West Sacramento, CA) at 37 °C in a humidified atmosphere of 5% CO_2. For subculture and experiments cells were washed with 1× DPBS (Cellgro, Mediatech, Mannassas, VA), detached using 0.025% Trypsin-EDTA (Cellgro, Mediatech, Mannassas, VA), collected in growth media and centrifuged. All experiments were performed in growth media using sub-confluent cells in the exponential growth phase.

2.2. Compounds

Stock solutions of all compounds were prepared in dimethylsulfoxide (DMSO) (EMD Chemicals, Gibbstown, NJ) and stored at −20 °C. Further

dilutions were made fresh in DPBS or cell-culture media. Gemcitabine hydrochloride and erlotinib hydrochloride were purchased from LKT Laboratories (St. Paul, MN) and LC Laboratories (Woburn, MA), respectively. Resveratrol, *N*-acetylcysteine and cell permeable glutathione (glutathione reduced ethyl ester) were bought from Sigma-Aldrich (St. Louis, MO). Sodium lipoate was purchased from GeroNova Research Inc. (Richmond, CA). Control samples in all the experiments were treated with vehicle (0.1% DMSO).

2.3. Measurement of cellular oxygen consumption

Cellular oxygen consumption rate was analyzed by using an XF 24 Extracellular Flux Analyzer (Seahorse Bioscience, Billerica, MA) as previously described [22]. Briefly, the assays were performed in a disposable sensor cartridge containing 24 pairs of fluorescent biosensors coupled to a fiberoptic waveguide, and a 24-well XF24 cell culture microplate.

The biosensor cartridge was prepared by hydrating with an XF24 calibrant solution (Seahorse Bioscience, Billerica, MA), and then incubating overnight at 37 °C in CO_2-free incubator. Simultaneously, cells were seeded (MDA-MB-435 120,000 cells/well; MIA PaCa-2 60,000 cells/well) in 100 μL culture medium in each well of the XF 24 cell microplate except A1, B4, C3 and D6 control wells. The cells were allowed to adhere for 6 h and then 150 μL of culture media was added to each well. The plate was then incubated overnight at 37 °C in the presence of 5% CO_2.

At the start of the experiment, the assay medium was warmed to 37 °C, and the pH was adjusted to 7.4. Culture medium was removed from the XF24 cell microplate, and the cells were washed using assay medium. After that, 600 μL of the assay medium was added to each well and the XF24 cell microplate was incubated at 37 °C for 1 h in a CO_2-free incubator. Concurrently, dilutions of all the compounds were prepared in assay media. 60 μL of the dilutions were added to the injection ports of the biosensor cartridge, and it was then maintained at 37 °C without CO_2 supplementation. Calibration and assay measurements were then performed at 37 °C using XF24.

2.3.1. Assay medium

DMEM base (8.3 g, Sigma-Aldrich, St. Louis, MO) and sodium chloride (1.85 g, Sigma-Aldrich, St. Louis, MO) were dissolved separately in 500 mL distilled water. The two solutions were then combined together and 20 mL of this combined solution was replaced with 10 mL of 100× GlutaMax-1 (Gibco, Invitrogen, Carlsbad, CA) and 10 mL of 100 mM sodium pyruvate (Sigma-Aldrich, St. Louis, MO). The complete medium was then warmed to 37 °C, and its pH was adjusted to 7.4 using 5 M sodium hydroxide (Sigma-Aldrich, St. Louis, MO). Finally, it was sterilized by filtration and stored at 4 °C for future use. Temperature and pH were again adjusted to 37 °C and 7.4 respectively on the day of the assay.

2.4. Cytotoxicity assay

Cytotoxicity was assessed by a 3-(4,5-dimethylthiazol-2-yl)-2,5-diphenyltetrazolium bromide (MTT) assay as previously described [26]. Briefly, cells were seeded in 96-well tissue culture treated plates and allowed to adhere overnight. Cells were subsequently treated with compounds or vehicle for the required amount of time. After 72 h, MTT (0.3 mg/mL) was added to each well. Cells were incubated with MTT for 3 h at 37 °C. After removal of the supernatant, DMSO was added and the absorbance was read at 570 nm. All assays were done in triplicate. % cytotoxicity was calculated by comparing the absorbance from drug treated wells to that of the control wells using the following formula: % cytotoxicity = 100 × (1 − [Abs (drug treated) / Abs (control)]). The IC_{50} was determined for each compound from a plot of log (drug concentration) versus percentage of cell kill.

2.5. Colony formation assay

Colony formation assay was performed as previously described [27]. Briefly, cells were seeded in 96 well tissue culture plates at a density of 200 cells per well (or in 6 well plates at a density of 250 cells per well) in growth media and allowed to adhere overnight. Cells were subsequently treated with different concentrations of compounds at various times. Following treatment, cells were washed with 1× DPBS and incubated in growth media for a period of 7–10 days, allowing sufficient time for colonies to form in control wells. To visualize the extent of colony formation, cells were fixed and stained in a 0.25% solution of crystal violet containing 10% formalin and 80% methanol. Excess stain was removed through multiple washes in distilled water and allowed to air dry. Stained plates were imaged using VersaDoc imaging platform (Bio-Rad Laboratories, Hercules, CA) and analyzed with Quantity One software (Bio-Rad Laboratories, Hercules, CA).

2.6. Superoxide detection

Superoxide production was quantified by measuring the rate of reduction of ferricytochrome *c* to ferrocytochrome *c* [28]. Briefly, cells were seeded in a 96-well plate at a density of 20,000 cells per well and allowed to adhere overnight. The next day, cells were treated with 5 μM of compounds **3a**–**c** (representative compounds of this class) with or without superoxide dismutase (20 U) (Sigma-Aldrich, St. Louis, MO). 125 μM of partially acetylated cytochrome c (Sigma-Aldrich, St. Louis) was added right before starting the measurements. The absorbance was measured every 5 min for 3 h at 550 nm. The initial rate was calculated by analyzing the change in absorbance with time.

2.7. Thiol detection

BxPC-3 (20,000 cells/well) and MIA PaCa-2 (20,000 cells/well) cells were seeded in a 96-well clear bottom black plate and allowed to adhere overnight. The next day cells were treated with increasing concentrations of compound **3b** for 4 h. Cells were then washed with 1× DPBS and stained with 1 μM CellTracker™ Green CMFDA (Invitrogen, Carlsbad, CA) for 45 min at 37 °C. Following which cells were incubated in fresh culture media for 30 min at 37 °C, washed with 1× DPBS, counterstained with DRAQ5® (Cell Signaling Technology, Danvers, MA). Cells were then fixed with 3.7% formaldehyde in 1× DPBS at 37 °C for 10 min, and then imaged using BD Pathway 435 High-Content Bioimager (BD Biosciences, San Jose, CA) at 10× magnification.

2.8. Western blotting

MIA PaCa-2 cells were seeded and allowed to adhere overnight. After the desired treatment, cells were washed with 1× DPBS and lysed using the RIPA lysis buffer (1% Nonidet P-40, 0.5% sodium deoxycholate, 0.1% SDS) in the presence of protease inhibitor (SIGMAFAST™ protease inhibitor cocktail tablet, EDTA-free, Sigma-Aldrich, St. Louis, MO) and phosphatase inhibitor (sodium orthovanadate, VWR International, Radnor, PA). Cell lysates were then sonicated and centrifuged at 12,000 rpm for 10 min at 4 °C. Protein concentration of the whole cell lysates was measured using BCA protein assay and equal amounts of total protein were resolved on a 10% polyacrylamide via SDS-PAGE. The separated proteins were electroblotted onto nitrocellulose membrane and blocked in 5% milk in TBST (Tris–Buffered Saline with Tween® 20) for 1 h at room temperature. The membrane was probed with primary antibodies to JNK, β-Tubulin (Santa Cruz Biotechnology Inc., Santa Cruz, CA), to p-p38, p38, p-JNK, GAPDH, p-Akt, Akt, p-FoxO3a, FoxO3a, p-H2AX, H2AX, c-Jun, p-c-Jun, FasL, Fas, cleaved caspase-8 and cleaved caspase 3 (Cell Signaling Technology, Danvers, MA), MnSOD and catalase (Sigma-Aldrich, St. Louis, MO)] at 4 °C overnight. Horseradish peroxidase-conjugated secondary antibodies (Santa Cruz Biotechnology Inc., Santa

Cruz, CA) in combination with SuperSignal West Dura (ThermoFisher Scientific, Waltham, MA) were used to visualize proteins of interest with a ChemiDoc Imaging system (Bio-Rad Laboratories, Hercules, CA). Quantification of bands was done using ImageJ software.

2.9. Statistics

Where indicated, *p*-values were calculated using Student's *t*-test. *p*-Values less than 0.05 were considered to be statistically significant.

2.10. Chemistry: General procedure for preparation of compounds and intermediates

A solution of quinazoline-5,8-dione (**1**, 1.0 mM for **3a**, 0.57 mM for **3b**–**d**, 0.62 mM for **3e**–**f**), cerium chloride ($CeCl_3 \cdot 7H_2O$) (1.1 eq), and aminoacylbenzene (**2a**–**f**, 1.1 eq) in absolute ethanol (15 mL for **3a**, 10 mL for **3b**–**f**), pre-saturated with oxygen, was stirred at room temperature (rt) for 5 h. Then, most of the ethanol was removed under vacuum, and water was added, followed by extraction of the mixture with chloroform ($CHCl_3$). The organic layers were dried over sodium sulfate (Na_2SO_4) and concentrated to dryness. The crude product was purified by flash chromatography (eluent: ethyl acetate) to give the desired compound.

The synthesis of compounds **3a**–**f** and **4** (Supplementary Schemes A1 and A2) was carried out using Bracher's methodology [29]. Regioselective substitution of quinazoline-5,8-dione **(1)** with appropriate aminoacylbenzene (**2a**–**f**) in the presence of Ce(III) ions gave **3a**–**f**. The acid-catalyzed cyclization of **3a** led to the formation of the condensed product **4**.

Supplementary Scheme A3 illustrates the synthesis of the key synthone **1** from readily available dimethoxybenzaldehyde **5**. Nitration of compound **5** with a molar excess of silica gel supported nitric acid, under simple magnetic stirring or by ultrasonic agitation, afforded the 3,6-dimethoxy-2-nitrobenzaldehyde (**6**). The latter was converted to diformamido-derivative **7**, which was then cyclized to give dimethoxyquinazoline **8**. Final oxidation by cerium ammonium nitrate resulted in the production of quinazoline-5,8-dione **1**.

It has been reported that amines attack the 6- and 7-positions of the isostere quinolin-5,8-dione, and the regioselectivity depends on the charge density at these positions. Additionally, the acid medium and Ce^{3+} ions increase 6-amino derivative formation [30]. We performed X-ray crystallographic studies to prove the regiochemistry of coupling between the aminoacetophenone **2a** and the quinone **1** in 6-position of the quinazolinedione ring (Supplementary Fig. A5 and Supplementary Tables A2, A3, A4). Elemental analyses for compounds **3a**–**f** and **4** are reported in Supplementary Table A5 (a detailed synthesis of the intermediates is mentioned in the supplementary section).

6-[(2-acetylphenyl)amino]quinazoline-5,8-dione (3a). Red–brown solid. Yield: 56%; mp 206–209 °C. IR (KBr): ν cm^{-1} 3315, 1685. ^1H NMR ($CDCl_3$): δ 11.40 (s, 1H, NH), 9.67 (s, 1H, H_4), 9.54 (s, 1H, H_2), 8.01 (d, 1H, Ar–H), 7.64 (d, 2H, Ar–H), 7.32–7.24 (m, 1H, Ar–H), 6.99 (s, 1H, H_7), 2.71 (s, 3H, CH_3). ^{13}C NMR ($CDCl_3$): δ 201.5, 181.2, 180.3, 163.5, 156.7, 143.6, 139.1, 134.3, 132.4, 126.1, 124.1, 123.4, 121.0, 107.2, 28.5. MS: *m/z* 293 (M^+). Anal. ($C_{16}H_{11}N_3O_3$) C, H, N.

6-[(3-acetylphenyl)amino]quinazoline-5,8-dione (3b). Red–brown solid. Yield: 67%; mp 215–218 °C. IR (KBr): ν cm^{-1} 3315, 1685. ^1H NMR ($CDCl_3$): δ 9.68 (s, 1H, H_4), 9.52 (s, 1H, H_2), 7.87 (d, 1H, Ar–H), 7.67–7.54 (m, 3H, Ar–H), 6.62 (s, 1H, H_7), 2.65 (s, 3H, CH_3). MS: *m/z* 293 (M^+). Anal. ($C_{16}H_{11}N_3O_3$) C, H, N.

6-[(4-acetylphenyl)amino]quinazoline-5,8-dione (3c). Red–brown solid. Yield: 67%; mp 228–230 °C. IR (KBr): ν cm^{-1} 3315, 1685. ^1H NMR ($CDCl_3$): δ 9.69 (s, 1H, H_4), 9.53 (s, 1H, H_2), 8.06 (d, 2H, Ar–H), 7.39 (d, 2H, Ar–H), 6.83 (s, 1H, H_7), 2.63 (s, 3H, CH_3). MS: *m/z* 293 (M^+). Anal. ($C_{16}H_{11}N_3O_3$) C, H, N.

6-{[2-(phenylcarbonyl)phenyl]amino}quinazoline-5,8-dione (3d). Red–brown solid. Yield: 77%; mp 167–170 °C. IR (KBr): ν cm^{-1} 3320, 1680. ^1H NMR ($CDCl_3$): δ 10.46 (bs, 1H, NH), 9.66 (s, 1H, H_4), 9.51 (s, 1H, H_2), 7.83–7.50 (m, 9H, Ar–H), 6.92 (s, 1H, H_7). MS: *m/z* 355 (M^+). Anal. ($C_{21}H_{13}N_3O_3$) C, H, N.

6-{[3-(phenylcarbonyl)phenyl]amino}quinazoline-5,8-dione (3e). Red–brown solid. Yield: 82%; mp 196–199 °C. IR (KBr): ν cm^{-1} 3320, 1680. ^1H NMR ($CDCl_3$): δ 10.40 (bs, 1H, NH), 9.67 (s, 1H, H_4), 9.51 (s, 1H, H_2), 7.82 (d, 1H, Ar–H), 7.73–7.50 (m, 8H, Ar–H), 6.67 (s, 1H, H_7). MS: *m/z* 355 (M^+). Anal. ($C_{21}H_{13}N_3O_3$) C, H, N.

6-{[4-(phenylcarbonyl)phenyl]amino}quinazoline-5,8-dione (3f). Red–brown solid. Yield: 73%; mp 233–236 °C. IR (KBr): ν cm^{-1} 3320, 1680. ^1H NMR ($CDCl_3$): δ 10.42 (bs, 1H, NH), 9.69 (s, 1H, H_4), 9.53 (d, 1H, H_2), 7.93 (d, 1H, Ar–H), 7.80 (d, 1H, Ar–H), 7.64–7.49 (m, 6H, Ar–H), 7.42 (d, 1H, Ar–H)ò. MS: *m/z* 355 (M^+). Anal. ($C_{21}H_{13}N_3O_3$) C, H, N.

11-Methylpyrimido[4,5-b]acridine-5,12-dione (4). Yellowish brown solid. Yield: 25%; mp ≥280 °C; IR (KBr): ν cm^{-1} = 1685. ^1H-NMR ($CDCl_3$): δ 9.84 (s, 1H, H_4), 9.78 (s, 1H, H_2), 8.47 (m, 2H, Ar–H), 8.01 (m, 1H, Ar–H), 7.86 (m, 1H, Ar–H), 3.35 (s, 3H, CH_3). MS: *m/z* 275 (M^+). Anal. ($C_{16}H_9N_3O_2$) C, H, N.

3. Results

3.1. Compound 3a increases cellular OCR

Compound **3a** was discovered in a random medium throughput screen of a highly diverse in-house library of ~1000 drug-like small-molecule compounds for their effects on cellular bioenergetics. **3a** resulted in immediate (first measurement was taken at 9 min after compound addition), and significant increase in cellular OCR in cancer cells. Furthermore, **3a** promoted 3-fold increase in cellular OCR as compared to resveratrol and lipoic acid (Fig. 2A). Resveratrol and lipoic acid are compounds that are being investigated for their anticancer potential. They are also known to enhance oxygen consumption in cells [31–35].

Further structural optimization of **3a** led to a series of analogs (Table 1) with varying degrees of effect on cellular OCR. All these analogs exhibit favorable drug like properties (Table 2). The analogs were designed with a bulky benzophenone or a smaller acetophenone group attached to the *N* on the 6-position of quinazoline-5,8-dione, or by ring closure at that position. Compounds with closed ring system (**4**) or bulkier groups (**3d**, **3f**) exerted less effect on OCR. Moreover, *meta* substitution was the most effective substitution (compounds **3b** and **3e**). Compound **3e** even with a bulkier benzophenone group (also present in **3d**, **3f**) showed similar activity as compound **3b**.

Compound **3b** was the most potent analog of **3a**, which resulted in 11-fold increase in cellular OCR (Fig. 2B, C). Therefore, we used compound **3b** as a representative of this class of compounds for further studies. Furthermore, **3b** induced dose dependent increase in cellular OCR (Fig. 2D, E). Moreover, the OCR inducing effects were not seen in the absence of cells (data not shown), suggesting that the cell signaling machinery is crucial for **3b** and its analogs to exert their effects.

3.2. Mitochondrial inhibitors do not abolish the OCR increasing effects of compound 3b

Mitochondria and cell metabolism play a vital role in regulating cellular bioenergetics and redox status. Therefore, we assessed for any changes in OCR increasing efficacy of compound **3b** in presence of mitochondrial inhibitors (Supplementary Fig. A1). Compound **3b** was able to increase cellular OCR in cells pretreated with oligomycin (ATP synthase inhibitor) or FCCP (mitochondrial uncoupler) (Supplementary Fig. A1A, B). However, the change in OCR right after the compound **3b**

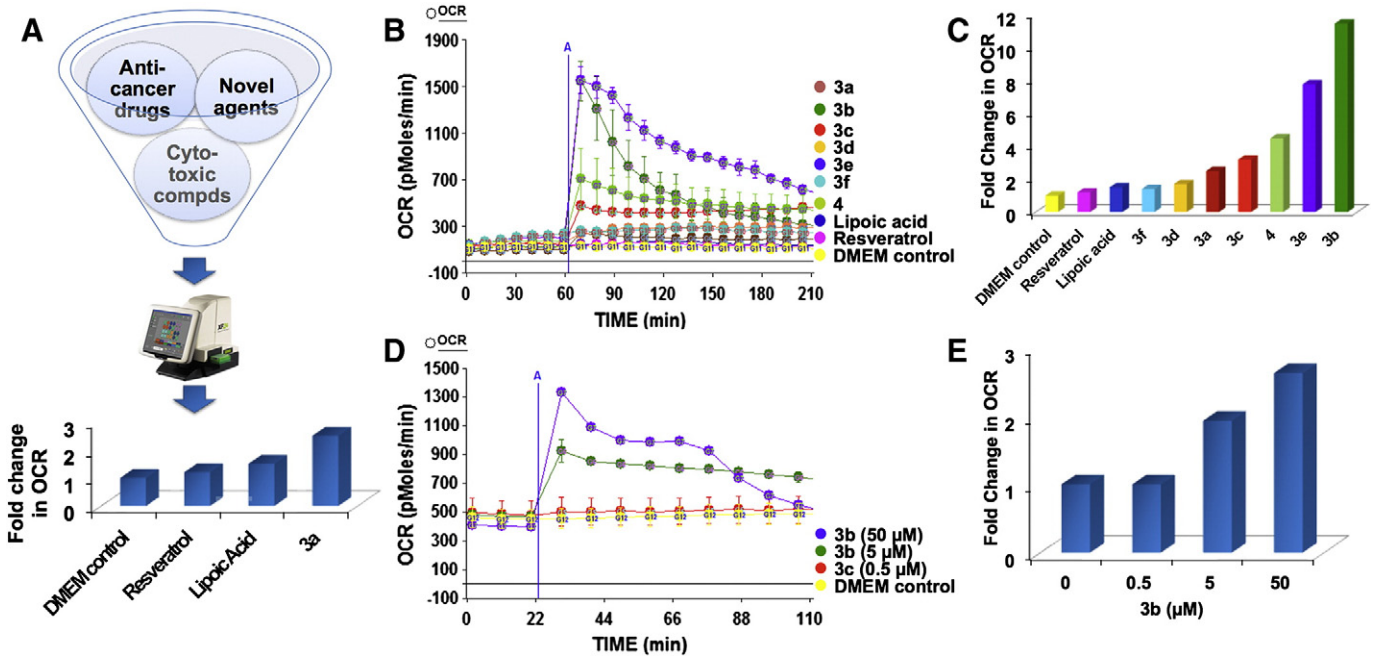

Fig. 2. Compounds **3a–f** and **4** induce significant increase in cellular oxygen consumption. (A) Compound **3a** was identified by a medium throughput screen of ~1000 highly diverse in-house compounds and chemotherapeutic agents using an XF24 Extracellular Flux Analyzer. **3a** (5 μM) induced 3-fold increase in cellular oxygen consumption in MDA-MB-435 cells when compared to resveratrol (50 μM) and lipoic acid (100 μM). (B) Structural optimization of compound **3a** led to discovery of 6 analogs. Compound **3b** (5 μM) was the most potent analog in increasing OCR in MDA-MB-435 cells. (C) Fold change increase in OCR was most significant for compound **3b**. (**3a–f**, 5 μM; **4**, 5 μM; Resveratrol, 50 μM; Lipoic acid (sodium lipoate) 100 μM) (D) Compound **3b** exerted a dose dependent increase in OCR in MIA PaCa-2 cells. (E) Quantification of data shown in (D) in terms of fold change (**3b**, 0.5 μM, 5 μM, 50 μM).

addition was slightly lower or higher in the cells pretreated with oligomycin or FCCP, respectively as compared to cells pretreated with medium control (DMEM). This difference can be attributed to the change in the basal OCR as a response to the addition of the mitochondrial inhibitor right before compound **3b** addition [*the change due to oligomycin* (*decrease*) *or FCCP* (*increase*) *treatment*]. Similar results were obtained with pretreatment with inhibitors of mitochondrial complexes (Supplementary Fig. A1C, D). Pretreatment with antimycin A (complex III inhibitor) or rotenone (complex I inhibitor) did not completely abolish the effects of compound **3b** on OCR.

3.3. Compounds 3a–f and 4 inhibit cell proliferation in human pancreatic cancer cells

Cytotoxicity of compounds **3a–f** and **4** was tested in a panel of pancreatic cancer cell lines by MTT assay (Table 1). All the compounds showed IC_{50} values in the low micromolar range in all cell lines.

Table 2
Druglikeliness of compounds **3a–f** and **4**.[a]

Compound	Mol. wt.[b]	miLogP[c]	HBD[d]	HBA[e]	No. of rotatable bonds[f]
3a	293.28	1.83	1	6	3
3b	293.28	1.85	1	6	3
3c	293.28	1.88	1	6	3
3d	355.35	3.39	1	6	4
3e	355.35	3.41	1	6	4
3f	355.35	3.43	1	6	4
4	275.27	2.17	0	5	0

[a] Druglikeliness of a compound is defined by its ability to follow Lipinski's rule of five. These properties were calculated using www.molinspiration.com.
[b] Mol. wt. should be 500 Da or less.
[c] miLogP refers to Log P calculated by molinspiration (mi). Log P is the measure of lipophilicity of the compound and should be 5 or less.
[d] HBD refers to number of hydrogen bond donors in the molecule. HBD should be 5 or less.
[e] HBA refers to number of hydrogen bond acceptors in the molecule. HBA should be 10 or less.
[f] No. of rotatable bonds should be 10 or less.

However, lower potencies were observed for compounds **3d** in BxPC-3, MIA PaCa-2 and PANC-1, **3e** in MIA PaCa-2 and BxPC-3, and **3f** in BxPC-3, suggesting that the addition of a bulkier group (**3d**, **3e**, **3f**) decreased their activity. Similar results were obtained in the colony formation assays where cells were treated for 24 h with the compounds (Supplementary Fig. A2D). More importantly, all our novel compounds are more potent than erlotinib, one of the standard clinically used drugs for pancreatic cancer (erlotinib, an EGFR inhibitor acts a multikinase inhibitor in pancreatic ductal adenocarcinomas, and in combination with gemcitabine was approved in 2005 for treatment of pancreatic cancer [36,37]). Moreover, these compounds are more potent than resveratrol and lipoic acid that are known inducers of OCR and are being developed as anticancer agents (Table 1) [31–35].

Furthermore, these compounds inhibit cell proliferation in breast, colon, prostate, ovarian and lung cancer cell lines (Supplementary Table A1). The inhibition of cell proliferation obtained by MTT assay was confirmed by colony formation assay (Supplementary Fig. A3). Interestingly, these compounds exert similar activity in HCT 116 $p53^{+/+}$ and HCT 116 $p53^{-/-}$, suggesting that their mode of action might be independent of p53 expression. More importantly, all compounds were potent in adriamycin-resistant NCI/ADR-RES cells overexpressing MDR-1 [38] and in HEY cells that are inherently resistant to cisplatin [23,24]. Therefore, compound **3b** and its analogs have great potential for treating resistant forms of cancer and warrant further investigation.

3.4. Compounds 3a–c induce oxidative stress in cancer cells

Our novel quinazolinediones significantly increased cellular OCR and potently inhibited cancer cell proliferation. Increased oxygen consumption by the treated cells might increase cellular ROS levels resulting in ROS-mediated cell death. To test this hypothesis we evaluated superoxide production upon treatment with these compounds using the partially-acetylated cytochrome c assay. This assay is based on the ability of superoxide to reduce the partially-acetylated cytochrome c [28]. Addition of compound **3b** and its closest analogs (**3a**, **3c**) resulted in immediate (first measurement at 5 min after

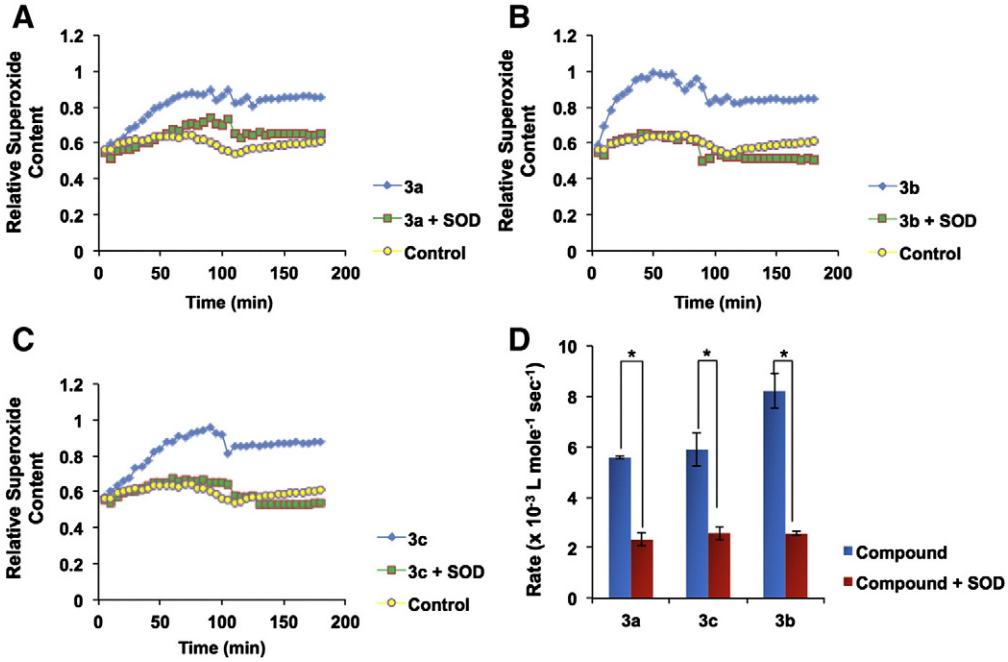

Fig. 3. Compounds **3a–3c** induce immediate and significant increase in superoxide production in MIA PaCa-2 pancreatic cancer cells. Compounds **3a** (A), **3b** (B), and **3c** (C) cause significant increase in superoxide production. Cells treated with compounds **3a–c** (blue); Cells treated with compounds **3a–c** in presence of superoxide dismutase (green); Control cells treated with partially acetylated cytochrome c (yellow). (D) Rate of superoxide generation calculated from the curves shown in A, B and C. (**3a–c**, 5 μM; SOD, 20 U; partially acetylated cytochrome c, 125 μM. *Indicates $p < 0.05$).

compound addition) and sustained (lasting 3 h) increase in superoxide production (Fig. 3A, B, C). The initial rate of superoxide generation was highest in cells treated with compound **3b**, the most potent analog, corroborating the results obtained from XF24's screening (Fig. 3D).

Mitochondria are the major source of cellular ROS production and are implicated in the process of "ROS-induced ROS release" [39]. ROS produced by a mitochondrion or any other cellular source are capable of stimulating ROS production in another mitochondrion initiating a chain reaction of ROS generation [40]. Therefore, we investigated the ability of **3b** to generate mitochondrial ROS using MitoSOX Red, a mitochondrial targeted probe that undergoes oxidation in the presence of superoxide giving rise to a fluorescent product. Treatment with **3b** resulted in a significant increase in mitochondrial superoxide in a time- and dose-dependent manner in all three pancreatic cancer cell lines tested (Supplementary Fig. A4).

Furthermore, depletion of cellular antioxidants' pool can make cancer cells more susceptible to oxidative stress induced cell death [16]. Therefore, we tested the effect of **3b** on the levels of cellular

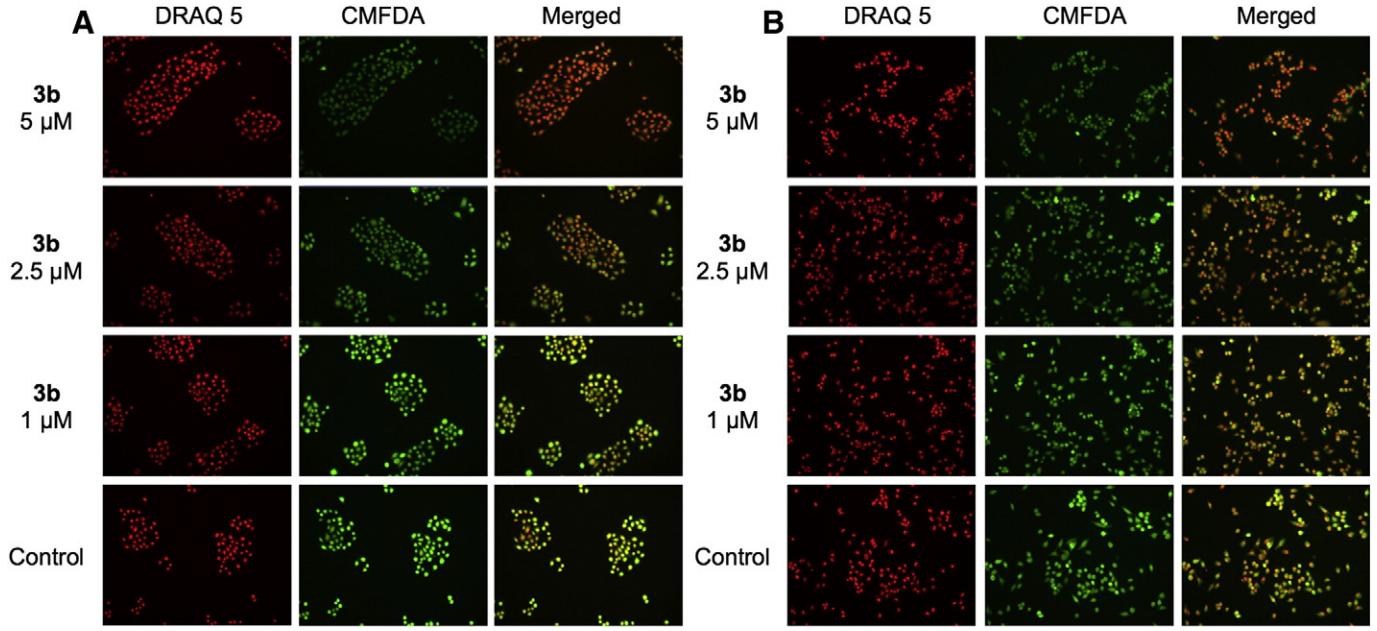

Fig. 4. Compounds **3b** depletes cellular antioxidants in pancreatic cancer cells. BxPC-3 (20,000 cells/well) and MIA PaCa-2 (20,000 cells/well) cells were treated with increasing concentrations of compound **3b** (1 μM, 2.5 μM and 5 μM) for 4 h. Treatment of (A) BxPC-3 and (B) MIA PaCa-2 cells with compound **3b** resulted in decrease in cellular glutathione content in a dose dependent manner (CellTracker Green™ CMFDA stains for cellular glutathione, DRAQ5® is the nuclear stain).

antioxidants. As expected, treatment with **3b** depleted cellular thiols (Fig. 4). Cells treated with compound **3b** (5 μM, 2.5 μM and 1 μM) for 4 h and then exposed to Cell Tracker Green™ CMFDA for ~1 h exhibited decreased signal intensity as compared to control, suggesting depletion of cellular thiols (Fig.4).

3.5. Compounds **3a**–**f** and **4** induce rapid inhibition of cancer cell proliferation

Compounds **3a**–**3f** and **4** increased cellular oxygen consumption and superoxide production in pancreatic cancer cells within minutes (Fig. 2, 3 and Supplementary Fig. A4). Therefore, we investigated their cytotoxic potential using shorter drug treatments in the colony formation and the MTT assays. In agreement with the above results, 10 min treatments with **3b** followed by removal of drug, was sufficient to inhibit cell proliferation in BxPC-3, MIA Paca-2 and PANC-1 cells, indicating that **3b** has a rapid and irreversible mechanism of action (Fig. 5, Supplementary Fig. A2). Furthermore, **3b** was most potent in MIA Paca-2 cells with an IC_{50} of 8.7 ± 0.6 μM with just 30 min of drug exposure as determined by MTT assay (Fig. 5B). Therefore, we used MIA Paca-2 cells for all our further studies. Similar results were observed for all analogs indicating that these compounds have immediate and sustained inhibitory effects on cancer cell proliferation (Supplementary Fig. A2). Compounds **3a**–**3c** are more potent than compounds **3d**–**3f** and **4** supporting the results obtained in OCR experiments. Furthermore, the cytotoxic potential of lead compound **3b** was compared with that of gemcitabine in normal fibroblasts. The extent of cytotoxic effects exerted by compound **3b** in normal fibroblasts HFF-1 cells was similar to the toxicity induced by gemcitabine in these cells (data not shown).

3.6. Antioxidants overcome the cytotoxic effects of compound **3b**

On the basis of the data presented thus far we hypothesize that the cytotoxic effects of quinazolinediones on cancer cells are mediated by the production of ROS. To test this hypothesis we treated pancreatic cancer cells with compound **3b** in the presence or absence of antioxidants (*N*-acetylcysteine, NAC or glutathione reduced ethyl ester, cell permeable glutathione, GSH). Cells were pretreated with 0, 1 or 5 mM of NAC or GSH for 2 h followed by treatment with compound **3b** at 5 μM for 72 h**.** Cells treated with compound **3b** in the presence of an antioxidant showed increased survival in a dose dependent manner as

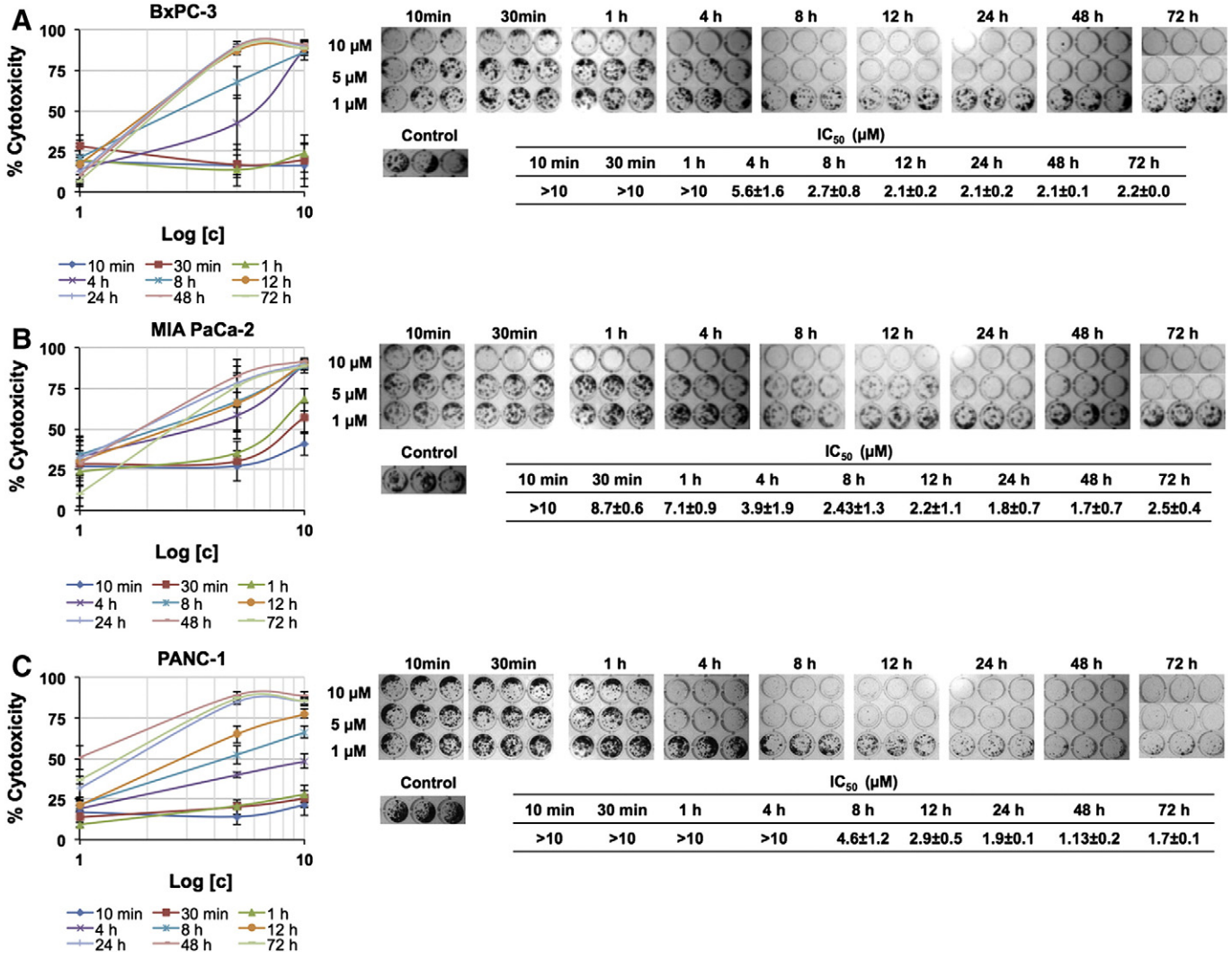

Fig. 5. Treatment with compound **3b** results in rapid inhibition of cancer cell proliferation. Colony formation and MTT assays were performed using compound **3b** in BxPC-3 (A), MIA PaCa-2 (B) and PANC-1 (C) cells. Cells were treated with a range of concentrations (1 μM, 5 μM and 10 μM) for increasing time periods (10 min, 30 min, 1 h, 4 h, 8 h, 12 h, 24 h, 48 h and 72 h), washed with 1× DPBS and allowed to grow into colonies in drug-free media for 5 days (MIA PaCa-2 cells), 7 days (PANC-1 cells) and 10 days (BxPC-3 cells), or incubated for 72 h MTT assay after the wash. The colonies obtained were stained using crystal violet and then imaged using VersaDoc imaging platform. (Curves represent the data generated from MTT assay. Inset tables show the IC_{50} values from MTT assay performed for a total of 72 h.)

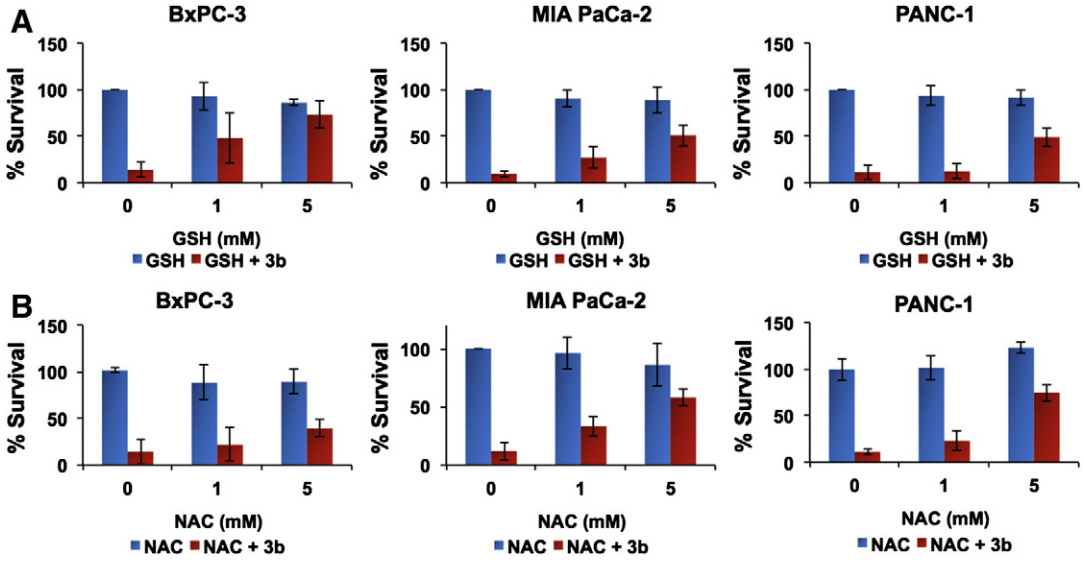

Fig. 6. Treatment with compound **3b** causes ROS-mediated cell death in pancreatic cancer cells. Treatment with antioxidants (A) Glutathione (GSH, cell permeable analog) or (B) *N*-acetylcysteine (NAC) increases survival of pancreatic cancer cells treated with **3b**. X-axis represents the concentration of antioxidant in mM (0, 1 and 5). Blue bars represent % survival in cells treated with antioxidant alone. Red bars represent cells pre-treated with the antioxidant for 2 h and then treated with compound **3b** (5 μM) for a total of 72 h. Results are obtained from MTT based cytotoxicity assay.

compared to cells treated with compound **3b** alone, confirming a ROS-mediated cell death mechanism for these compounds (Fig. 6).

3.7. Compound **3b** promotes Akt-directed increase in cellular ROS

Previously, it has been shown that Akt increases intracellular ROS by increasing oxygen consumption and decreasing ROS scavenging [41]. Similarly, compound **3b** increases cellular OCR (Fig. 2) and induces cellular superoxide generation (Fig. 3 and Supplementary Fig. A4). Therefore, we postulated that the ROS-mediated cell death by compound **3b** may be due to Akt activation. To test this hypothesis, MIA PaCa-2 pancreatic cancer cells were treated with compound **3b** (5 μM) at various time points. We observed a robust phosphorylation of Akt at S473 and T308 as early as 10 min. Activated Akt in turn phosphorylated its downstream target, FoxO3a (forkhead box O3a). However, phosphorylation of FoxO3a by Akt results in its inactivation and thus decreased expression of its target antioxidant enzymes [manganese superoxide dismutase (MnSOD) and catalase] (Fig. 7A). Mechanistically, compound **3b** causes a rapid increase in ROS upon treatment and a subsequent decrease of antioxidants' expression in cells between 8 and 12 h (Fig. 7A) suggesting that compound **3b** promotes Akt-directed oxidative stress in MIA PaCa-2 cells.

3.8. Compound **3b** activates stress kinases and causes apoptosis

The stress response caused by **3b** is supported by the early activation (10 min) of stress induced protein kinases, p38, and JNK and its downstream target c-Jun (Fig. 8A). Activated p38 and JNK have been implicated

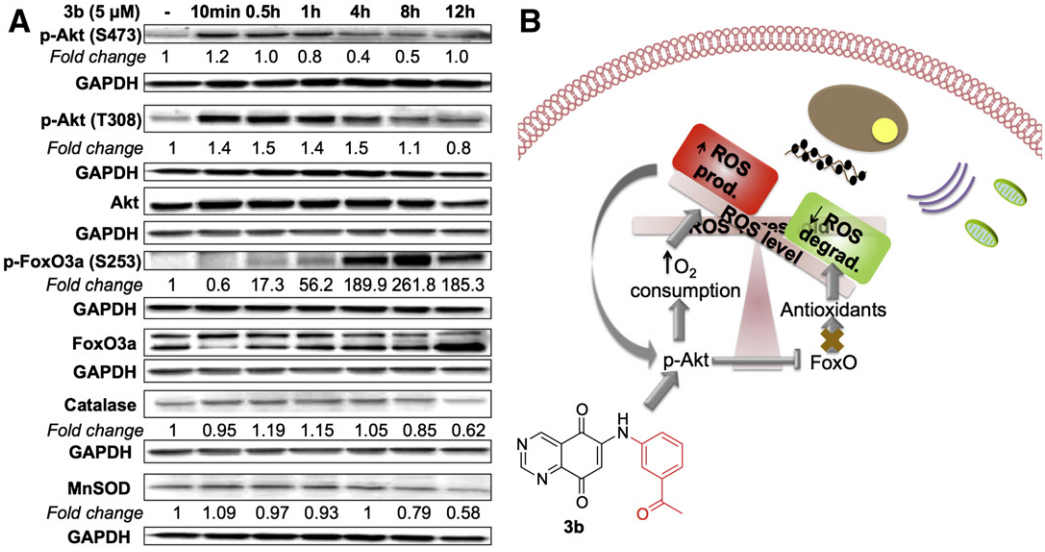

Fig. 7. Compound **3b** promotes Akt-directed increase in cellular oxidative stress. (A) Treatment with compound **3b** resulted in activation of Akt by increased phosphorylation at S473 and T308. Activated Akt phosphorylates FoxO3a (S253) resulting in its inactivation leading to decreased expression of its downstream target antioxidant enzymes manganese superoxide dismutase (MnSOD) and catalase. Thus, **3b** decreased the antioxidant content of cells. GAPDH was used as a loading control. (B) Compound **3b** induces ROS-mediated cell death in cancer cells. Treatment with compound **3b** resulted in Akt-directed increase in cellular oxygen consumption, ROS production, and decreased antioxidants' expression (MnSOD and catalase). Increased oxidative stress induced by **3b** overwhelms the adaptive capacity of cancer cells to survive at relatively higher basal ROS. Finally, increased cellular ROS resulted in activation of stress kinases and induction of cell death in cancer cells. Western blots were repeated at least thrice for each condition. Representative blots are shown in here. Quantification is done using ImageJ software. Total proteins were normalized to loading control. phospho-proteins were normalized to their loading control and then to their respective total protein content.

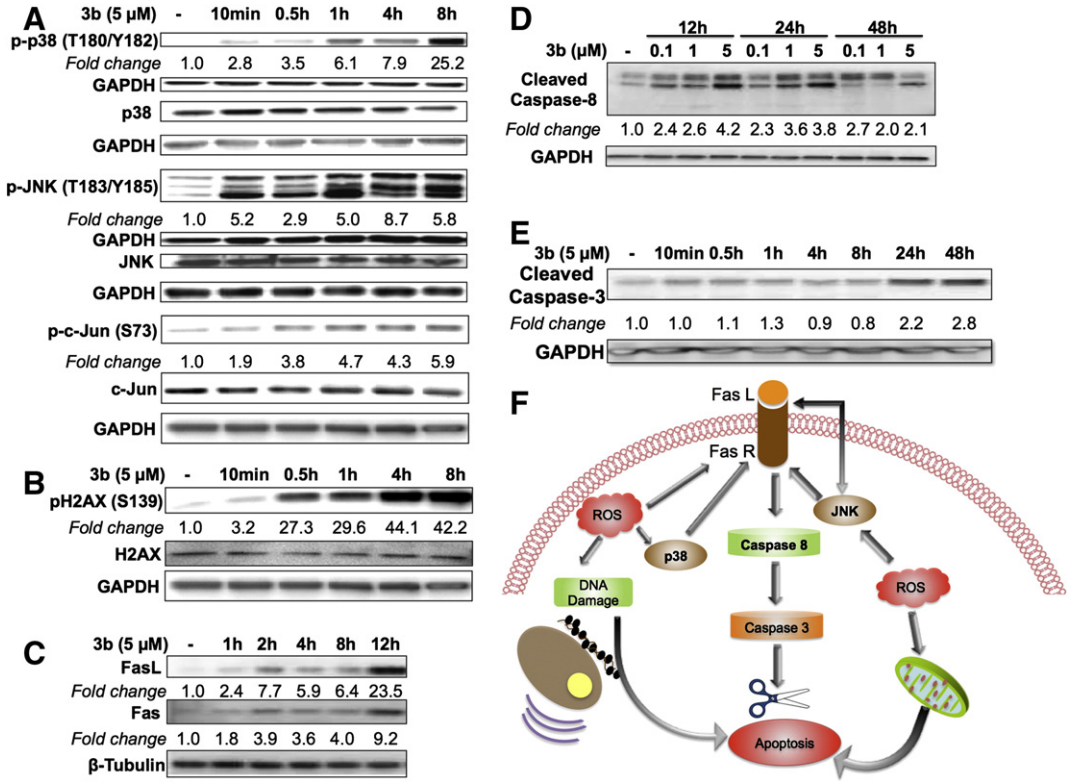

Fig. 8. Compound **3b** activates stress kinases and induces cell death in pancreatic cancer cells (A) **3b** treatment resulted in increased phosphorylation of stress kinases p38 (T180/Y182) and JNK (T183/Y185). Activated pJNK phosphorylates its downstream target c-Jun (S73). (B) Furthermore, treatment with compound **3b** also resulted in phosphorylation of H2AX (S139), a marker of DNA damage. (C) Oxidative stress results in increased expression of FasL, activation of Fas receptor and its downstream caspases (D, E). (F) Proposed mechanism: compound **3b** induced ROS-directed Fas-mediated apoptotic cell death in pancreatic cancer cells. Western blots were repeated at least thrice for each condition. Representative blots are shown here. Quantification is done using ImageJ software. Total proteins were normalized to loading control. phospho-proteins were normalized to their loading control and then to their respective total protein content.

in induction of cell death resulting from various forms of stress including oxidative stress [42–46]. DNA-damage was observed by a robust and sustained phosphorylation of histone H2AX at S139, a key marker for DNA double strand break (Fig. 8B). DNA double strand breaks can lead to apoptotic cell death [47]. Furthermore, treatment with compound **3b** activated Fas-mediated apoptotic signaling in pancreatic cancer cells (Fig. 8C, D, E). Thus, treatment with compound **3b** results in oxidative stress induced cell death in pancreatic cancer cells (Fig. 8F).

4. Discussion

6-Arylamino-7-chloro-quinazoline-5,8-diones have been reported as potential antitumor agents displaying DNA topoisomerase inhibitory properties resulting in their cytotoxic effects [48,49]. However, the quinazoline-5,8-diones mentioned in this paper structurally differ from the previously reported compounds in lacking 7-*chloro* substitution. Moreover, quinazoline-5,8-diones discovered by our group have an interesting mechanism of action on targeting the persistent oxidative stress in cancer cells. These compounds act by a rapid and sustained antiproliferative mechanism. These compounds induce rapid increase in cellular OCR and superoxide generation (Fig. 2, 3, Supplementary Fig. A4). Furthermore, **3b** depletes cellular thiols (Fig. 4) and aggravates cellular oxidative stress. A short exposure to the compound is adequate to induce cell death in cancer cells with sustained effects for ~10 days (Fig. 5). Additionally, these compounds potently inhibit cell proliferation in different cancer cell lines (Table 1, Supplementary Table A1, Fig. 5, Supplementary Fig. A2, A3). Importantly, they are active in both drug-sensitive and drug-resistant cancer cell lines. ROS-mediated anticancer therapy can overcome resistance associated with some anticancer agents. Expression of multidrug resistant transporter (p-glycoprotein) is dependent on intracellular ROS levels. For example, DU-145NOX1 (prostate cancer cell line over-expressing NADPH oxidase 1) has higher intracellular ROS and lower expression of P-gp as compared to DU-145 [20]. Since **3b** and its analogs exert activity in resistant cancer cell lines (HEY and NCI/ADR-RES), they would have great application in chemotherapy for resistant forms of cancer. Furthermore, **3b** exerts similar cytotoxic effects in normal fibroblasts HFF-1 cell line as compared to gemcitabine.

Akt is a pro-survival kinase that is upregulated in several forms of human cancers. Hyperactive Akt inhibits apoptosis induced by numerous stimuli. However, Akt is unable to inhibit ROS-mediated cell death, and in fact, Akt aids in ROS-directed cell death by inducing cellular oxygen consumption, promoting ROS generation, and impairing ROS degeneration. Akt mediates decreased ROS scavenging by phosphorylating the transcription factor FoxO causing its inactivation. This leads to decreased expression of its target antioxidant enzymes (MnSOD and catalase). Therefore, hyperactivated Akt sensitizes cancer cells to ROS-directed cell death [41]. Parthenolide, a sesquiterpene lactone, has been shown to induce Akt-directed ROS-mediated cell death in prostate cancer cells [50]. Compound **3b** increases Akt phosphorylation causing a decrease in FoxO3a activity that in turn reduces the cellular pool of antioxidants resulting in excessive oxidative stress in cancer cells (Fig. 7).

Increased oxidative stress activates stress kinases (p38/JNK) culminating in cancer cell death. Increased ROS generation by **3b** resulted in immediate and sustained activation of stress kinases' pathways (p38, JNK) that have been implicated in induction of cell death (Fig. 8A) [42,51,52]. Moreover, **3b** promoted H2AX phosphorylation in pancreatic cancer cells (Fig. 8B). H2AX is a marker for DNA damage and can be phosphorylated by JNK and p38, or under DNA damaging or oxidative stress conditions [53–55]. DNA damage can in turn lead to apoptosis [47]. Furthermore, ROS can lead to increased expression of FasL [56,57]. Additionally, activation of p38 and JNK by ROS has also been

implicated in Fas/FasL mediated apoptosis [58–60]. Treatment with compound **3b** resulted in increased expression and activation of Fas/FasL and the downstream caspases (caspase 8 and caspase 3) (Fig. 8C, D, E). Moreover, Fas can further activate JNK [61] and can intensify the cell death effect. Additionally, activated JNK can also migrate to mitochondria and induce mitochondrial apoptosis [59] and further aid in cell death initiated by ROS.

Due to limited therapeutic options for pancreatic cancer we plan to develop these compounds for pancreatic cancer treatment. Recent studies have shown that like most types of cancer, pancreatic cancer also exhibits increased oxidative stress [4]. Increased ROS in pancreatic cancer suggests the usefulness of ROS-mediated therapeutic strategy for this disease. Most forms of pancreatic cancer express over-activated mutated Ras. Ras oncogene can upregulate the expression of NOX1 (a homologue of catalytic subunit of superoxide producing enzyme, NADPH oxidase) and increase ROS generation [62]. Therefore, these compounds might be acting through Ras. However, since they have similar activities in Ras wt (BxPC-3) and mutated (MIA PaCa-2 and PANC-1) forms of cancer (Table 1), NOX1 does not seem a probable target for these compounds.

Additionally, pancreatic cancer cells have elevated expression of NAD(P)H:quinone oxidoreductase (NQO1), which detoxifies quinones. NQO1 reduces most quinones directly to hydroquinones, thus bypassing the highly reactive semi-quinone intermediate [63]. Dicumarol and ES936 inhibit NQO1 and demonstrate cytotoxic effects in pancreatic cancer [64,65]. However, certain agents like streptonigrin require NQO1 mediated activation for exerting cytotoxic effects [63,66]. Since these compounds have a quinone moiety, there is a possibility that NQO1 might be activating them like streptonigrin. Several other drugs like capsaicin, BITC and nitric oxide donating aspirin (NO-ASA) have shown ROS mediated cytotoxic effects in pancreatic cancer cell lines [67–69]. Moreover, pancreatic cancer cells are known to express activated Akt, which could aid in achieving Akt-directed ROS-mediated cell death in pancreatic cancer cells [70]. All these reports suggest that ROS mediated treatment is a rational approach for pancreatic cancer.

Lastly, these compounds have a quinone moiety in their structures, and most antitumor quinones undergo redox cycling (redox cycling: Quinone reductases catalyze one electron or two electron transfer reactions resulting in the formation of semiquinone and hydroquinone, respectively. Semiquinone reacts with oxygen, and generates superoxide and the parent quinone. Superoxide anion acts as a propagating species in the autoxidation of hydroquinones. NADPH cytochrome P450 reductase and NAD(P)H:quinone oxidoreductase are examples of one and two electron transfers catalyzing quinone reductases, respectively). Redox cycling of quinones is accompanied by consumption of oxygen, oxidation of NAD(P)H and formation of reactive oxygen species [71]. It is plausible that these compounds might be undergoing redox cycling inside cells resulting in increased superoxide generation and oxygen consumption. Therefore, they may be acted upon by one of the quinone reductases.

5. Conclusion

In conclusion, we have discovered a novel class of compounds displaying a unique mechanism of action. Compound **3b** and its analogs exert a significant increase in OCR in cells leading to ROS generation and cell death. This effect can be overcome by pre-treatment with antioxidants, validating the role of ROS in promoting cytotoxicity of **3b**. Therefore, with the discovery of compound **3b** we have provided compelling evidence in support of a hypothesis previously proposed by the Huang Lab "Targeting cancer cells by ROS-mediated mechanisms: a radical therapeutic approach?" [16].

High ROS levels could represent the Achilles' heel of cancer cells. Even though cancer cells have adapted to survive in an oxidative stress environment, exogenous oxidative insults can overwhelm the adaptive antioxidant capacity of cancer cells and trigger ROS-mediated cell death. Our novel class of quinazolinediones takes advantage of this weakness and by exacerbating oxygen consumption and reducing the antioxidant capacity of cancer cells they tip the balance towards activation of stress kinases that ultimately lead to cell death.

Supplementary data to this article can be found online at http://dx.doi.org/10.1016/j.bbagen.2013.08.005.

Acknowledgements

This study was supported in part by funds from the Sharon L. Cockrell Cancer Research Fund to NN and by financial support from the Regione Autonoma della Sardegna (grant CRP-25920), within the frame of "Legge regionale n. 7/2007, promozione della ricerca scientifica e dell'innovazione tecnologica in Sardegna, Annualità 2010", to MS. We thank A. Cosseddu for the help on the preparation of compounds, and M. Orecchioni and P. Fiori for the assistance with NMR spectroscopy. DP was a recipient of a USC Graduate School Oakley Fellowship.

References

[1] N.C.I. N. I. H., Pancreatic Cancer, (2013) http://www.cancer.gov/cancertopics/types/pancreatic/.
[2] D. Hanahan, R.A. Weinberg, Hallmarks of cancer: the next generation, Cell 144 (2011) 646–674.
[3] D. Pathania, M. Millard, N. Neamati, Opportunities in discovery and delivery of anticancer drugs targeting mitochondria and cancer cell metabolism, Adv. Drug Deliv. Rev. 61 (2009) 1250–1275.
[4] L. MacMillan-Crow, J. Greendorfer, S. Vickers, J. Thompson, Tyrosine nitration of c-SRC tyrosine kinase in human pancreatic ductal adenocarcinoma, Arch. Biochem. Biophys. 377 (2000) 350–356.
[5] F. Weinberg, N. Chandel, Reactive oxygen species-dependent signaling regulates cancer, Cell Mol. Life Sci. 66 (2009) 3663–3673.
[6] P. Storz, Reactive oxygen species in tumor progression, Front. Biosci. 10 (2005) 1881–1896.
[7] R. Shackelford, W. Kaufmann, R. Paules, Oxidative stress and cell cycle checkpoint function, Free Radic. Biol. Med. 28 (2000) 1387–1404.
[8] J. Boonstra, J.A. Post, Molecular events associated with reactive oxygen species and cell cycle progression in mammalian cells, Gene 337 (2004) 1–13.
[9] L. Behrend, G. Henderson, R. Zwacka, Reactive oxygen species in oncogenic transformation, Biochem. Soc. Trans. 31 (2003) 1441–1444.
[10] D. Kang, N. Hamasaki, Mitochondrial oxidative stress and mitochondrial DNA, Clin. Chem. Lab. Med. 41 (2003) 1281–1288.
[11] W. Wu, The signaling mechanism of ROS in tumor progression, Cancer Metastasis Rev. 25 (2006) 695–705.
[12] A. Jackson, L. Loeb, The contribution of endogenous sources of DNA damage to the multiple mutations in cancer, Mutat. Res. 477 (2001) 7–21.
[13] N.C.I. N. I. H, Antioxidant and Cancer Prevention: Fact Sheet, (2012) http://www.cancer.gov/cancertopics/factsheet/prevention/antioxidants.
[14] B. Schneider, M. Kulesz-Martin, Destructive cycles: the role of genomic instability and adaptation in carcinogenesis, Carcinogenesis 25 (2004) 2033–2044.
[15] G. Perry, A. Raina, A. Nunomura, T. Wataya, L. Sayre, M. Smith, How important is oxidative damage? Lessons from Alzheimer's disease, Free Radic. Biol. Med. 28 (2000) 831–834.
[16] D. Trachootham, J. Alexandre, P. Huang, Targeting cancer cells by ROS-mediated mechanisms: a radical therapeutic approach? Nat. Rev. Drug Discov. 8 (2009) 579–591.
[17] H. Pelicano, D. Carney, P. Huang, ROS stress in cancer cells and therapeutic implications, Drug Resist. Updat. 7 (2004) 97–110.
[18] M. Valko, D. Leibfritz, J. Moncol, M. Cronin, M. Mazur, J. Telser, Free radicals and antioxidants in normal physiological functions and human disease, Int. J. Biochem. Cell Biol. 39 (2007) 44–84.
[19] Q. Kong, J.A. Beel, K.O. Lillehei, A threshold concept for cancer therapy, Med. Hypotheses 55 (2000) 29–35.
[20] M. Wartenberg, E. Hoffmann, H. Schwindt, F. Grünheck, J. Petros, J. Arnold, J. Hescheler, H. Sauer, Reactive oxygen species-linked regulation of the multidrug resistance transporter P-glycoprotein in Nox-1 overexpressing prostate tumor spheroids, FEBS Lett. 579 (2005) 4541–4549.
[21] P.T. Schumacker, Reactive oxygen species in cancer cells: live by the sword, die by the sword, Cancer Cell 10 (2006) 175–176.
[22] M. Millard, D. Pathania, Y. Shabaik, L. Taheri, J. Deng, N. Neamati, Preclinical evaluation of novel triphenylphosphonium salts with broad-spectrum activity, PLoS One 5 (2010).
[23] R. Buick, R. Pullano, J. Trent, Comparative properties of five human ovarian adenocarcinoma cell lines, Cancer Res. 45 (1985) 3668–3676.
[24] K. Hamaguchi, A. Godwin, M. Yakushiji, P. O'Dwyer, R. Ozols, T. Hamilton, Cross-resistance to diverse drugs is associated with primary cisplatin resistance in ovarian cancer cell lines, Cancer Res. 53 (1993) 5225–5232.
[25] M.L. Wang, R. Walsh, K.L. Robinson, J. Burchard, S.R. Bartz, M. Cleary, D.A. Galloway, C. Grandori, Gene expression signature of c-MYC-immortalized human fibroblasts

reveals loss of growth inhibitory response to TGFbeta, Cell Cycle 10 (2011) 2540–2548.
[26] J. Carmichael, W. DeGraff, A. Gazdar, J. Minna, J. Mitchell, Evaluation of a tetrazolium-based semiautomated colorimetric assay: assessment of chemosensitivity testing, Cancer Res. 47 (1987) 936–942.
[27] A. Munshi, M. Hobbs, R. Meyn, Clonogenic cell survival assay, Methods Mol. Med. 110 (2005) 21–28.
[28] A. Azzi, C. Montecucco, C. Richter, The use of acetylated ferricytochrome c for the detection of superoxide radicals produced in biological membranes, Biochem. Biophys. Res. Commun. 65 (1975) 597–603.
[29] F. Bracher, Total synthesis of the pentacyclic alkaloid ascididemin, Heterocycles 29 (1989) 2093–2095.
[30] Y.T. Pratt, Quinolinequinones. VI. Reactions with aromatic amines, J. Org. Chem. 27 (1962) 3905–3910.
[31] J.A. Baur, K.J. Pearson, N.L. Price, H.A. Jamieson, C. Lerin, A. Kalra, V.V. Prabhu, J.S. Allard, G. Lopez-Lluch, K. Lewis, P.J. Pistell, S. Poosala, K.G. Becker, O. Boss, D. Gwinn, M. Wang, S. Ramaswamy, K.W. Fishbein, R.G. Spencer, E.G. Lakatta, D. Le Couteur, R.J. Shaw, P. Navas, P. Puigserver, D.K. Ingram, R. de Cabo, D.A. Sinclair, Resveratrol improves health and survival of mice on a high-calorie diet, Nature 444 (2006) 337–342.
[32] T.M. Hagen, R.T. Ingersoll, J. Lykkesfeldt, J. Liu, C.M. Wehr, V. Vinarsky, J.C. Bartholomew, A.B.. Ames, (R)-alpha-lipoic acid-supplemented old rats have improved mitochondrial function, decreased oxidative damage, and increased metabolic rate, FASEB J. 13 (1999) 411–418.
[33] J.I. Kim, S.R. Cho, C.M. Lee, E.S. Park, K.N. Kim, H.C. Kim, H.Y. Lee, Induction of ER stress-mediated apoptosis by α-lipoic acid in A549 cell lines, Korean J. Thorac. Cardiovasc. Surg. 45 (2012) 1–10.
[34] J.H. Zhou, H.Y. Cheng, Z.Q. Yu, D.W. He, Z. Pan, D.T. Yang, Resveratrol induces apoptosis in pancreatic cancer cells, Chin. Med. J. (Engl.) 124 (2011) 1695–1699.
[35] M. Jang, L. Cai, G.O. Udeani, K.V. Slowing, C.F. Thomas, C.W. Beecher, H.H. Fong, N.R. Farnsworth, A.D. Kinghorn, R.G. Mehta, R.C. Moon, J.M. Pezzuto, Cancer chemopreventive activity of resveratrol, a natural product derived from grapes, Science 275 (1997) 218–220.
[36] L. Conradt, K. Godl, C. Schaab, A. Tebbe, S. Eser, S. Diersch, C.W. Michalski, J. Kleeff, A. Schnieke, R.M. Schmid, D. Saur, G. Schneider, Disclosure of erlotinib as a multikinase inhibitor in pancreatic ductal adenocarcinoma, Neoplasia 13 (2011) 1026–1034.
[37] N.C.I. N. I. H., FDA Approval for Erlotinib Hydrochloride, (2013) http://www.cancer.gov/cancertopics/druginfo/fda-erlotinib-hydrochloride#Anchor-Pancreati-44285.
[38] D.A. Scudiero, A. Monks, E.A. Sausville, Cell line designation change: multidrug-resistant cell line in the NCI anticancer screen, J. Natl. Cancer Inst. 90 (1998) 862.
[39] P. Jezek, L. Hlavatá, Mitochondria in homeostasis of reactive oxygen species in cell, tissues, and organism, Int. J. Biochem. Cell Biol. 37 (2005) 2478–2503.
[40] D. Zorov, M. Juhaszova, S. Sollott, et al., Mitochondrial ROS-induced ROS release: an update and review, Biochim. Biophys. Acta (1757) 509–517.
[41] V. Nogueira, Y. Park, C. Chen, P. Xu, M. Chen, I. Tonic, T. Unterman, N. Hay, Akt determines replicative senescence and oxidative or oncogenic premature senescence and sensitizes cells to oxidative apoptosis, Cancer Cell 14 (2008) 458–470.
[42] L. Chang, M. Karin, Mammalian MAP kinase signalling cascades, Nature 410 (2001) 37–40.
[43] M. Verheij, R. Bose, X.H. Lin, B. Yao, W.D. Jarvis, S. Grant, M.J. Birrer, E. Szabo, L.I. Zon, J.M. Kyriakis, A. Haimovitz-Friedman, Z. Fuks, R.N. Kolesnick, Requirement for ceramide-initiated SAPK/JNK signalling in stress-induced apoptosis, Nature 380 (1996) 75–79.
[44] M.H. Cobb, MAP kinase pathways, Prog. Biophys. Mol. Biol. 71 (1999) 479–500.
[45] C. Tournier, P. Hess, D.D. Yang, J. Xu, T.K. Turner, A. Nimnual, D. Bar-Sagi, S.N. Jones, R.A. Flavell, R.J. Davis, Requirement of JNK for stress-induced activation of the cytochrome c-mediated death pathway, Science 288 (2000) 870–874.
[46] R.J. Davis, Signal transduction by the JNK group of MAP kinases, Cell 103 (2000) 239–252.
[47] W.P. Roos, B. Kaina, DNA damage-induced cell death by apoptosis, Trends Mol. Med. 12 (2006) 440–450.
[48] H.J. Park, Y.S. Kim, J.S. Kim, E.J. Lee, Y.J. Yi, H.J. Hwang, M.E. Suh, C.K. Ryu, S.K. Lee, 6-Arylamino-7-chloro-quinazoline-5,8-diones as novel cytotoxic and DNA topoisomerase inhibitory agents, Bioorg. Med. Chem. Lett. 14 (2004) 3385–3388.
[49] I. Choi, C. Kim, S. Choi, Binding mode analysis of topoisomerase inhibitors, 6-arylamino-7-chloro-quinazoline-5,8-diones, within the cleavable complex of human topoisomerase I and DNA, Arch. Pharm. Res. 30 (2007) 1526–1535.
[50] Y. Sun, D.K. St Clair, Y. Xu, P.A. Crooks, W.H. St Clair, A NADPH oxidase-dependent redox signaling pathway mediates the selective radiosensitization effect of parthenolide in prostate cancer cells, Cancer Res. 70 (2010) 2880–2890.
[51] H.M. Shen, Z.G. Liu, JNK signaling pathway is a key modulator in cell death mediated by reactive oxygen and nitrogen species, Free Radic. Biol. Med. 40 (2006) 928–939.
[52] Y.K. Lee, J.T. Hwang, D.Y. Kwon, Y.J. Surh, O.J. Park, Induction of apoptosis by quercetin is mediated through AMPKalpha1/ASK1/p38 pathway, Cancer Lett. 292 (2010) 228–236.
[53] C. Lu, Y. Shi, Z. Wang, Z. Song, M. Zhu, Q. Cai, T. Chen, Serum starvation induces H2AX phosphorylation to regulate apoptosis via p38 MAPK pathway, FEBS Lett. 582 (2008) 2703–2708.
[54] C. Lu, F. Zhu, Y.Y. Cho, F. Tang, T. Zykova, W.Y. Ma, A.M. Bode, Z. Dong, Cell apoptosis: requirement of H2AX in DNA ladder formation, but not for the activation of caspase-3, Mol. Cell. 23 (2006) 121–132.
[55] Z. Li, J. Yang, H. Huang, Oxidative stress induces H2AX phosphorylation in human spermatozoa, FEBS Lett. 580 (2006) 6161–6168.
[56] M.K. Bauer, M. Vogt, M. Los, J. Siegel, S. Wesselborg, K. Schulze-Osthoff, Role of reactive oxygen intermediates in activation-induced CD95 (APO-1/Fas) ligand expression, J. Biol. Chem. 273 (1998) 8048–8055.
[57] M. Suzuki, K. Aoshiba, A. Nagai, Oxidative stress increases Fas ligand expression in endothelial cells, J. Inflamm. (Lond.) 3 (2006) 11.
[58] W.H. Liu, Y.C. Cheng, L.S. Chang, ROS-mediated p38alpha MAPK activation and ERK inactivation responsible for upregulation of Fas and FasL and autocrine Fas-mediated cell death in Taiwan cobra phospholipase A(2)-treated U937 cells, J. Cell. Physiol. 219 (2009) 642–651.
[59] M.L. Circu, T.Y. Aw, Reactive oxygen species, cellular redox systems, and apoptosis, Free Radic. Biol. Med. 48 (2010) 749–762.
[60] J. Chandra, A. Samali, S. Orrenius, Triggering and modulation of apoptosis by oxidative stress, Free Radic. Biol. Med. 29 (2000) 323–333.
[61] D.J. Wilson, K.A. Fortner, D.H. Lynch, R.R. Mattingly, I.G. Macara, J.A. Posada, R.C. Budd, JNK, but not MAPK, activation is associated with Fas-mediated apoptosis in human T cells, Eur. J. Immunol. 26 (1996) 989–994.
[62] J. Mitsushita, J.D. Lambeth, T. Kamata, The superoxide-generating oxidase Nox1 is functionally required for Ras oncogene transformation, Cancer Res. 64 (2004) 3580–3585.
[63] A.M. Lewis, M. Ough, M.M. Hinkhouse, M.S. Tsao, L.W. Oberley, J.J. Cullen, Targeting NAD(P)H:quinone oxidoreductase (NQO1) in pancreatic cancer, Mol. Carcinog. 43 (2005) 215–224.
[64] D.L. Dehn, D. Siegel, K.S. Zafar, P. Reigan, E. Swann, C.J. Moody, D. Ross, 5-Methoxy-1,2-dimethyl-3-[(4-nitrophenoxy)methyl]indole-4,7-dione, a mechanism-based inhibitor of NAD(P)H:quinone oxidoreductase 1, exhibits activity against human pancreatic cancer in vitro and in vivo, Mol. Cancer Ther. 5 (2006) 1702–1709.
[65] P. Reigan, M.A. Colucci, D. Siegel, A. Chilloux, C.J. Moody, D. Ross, Development of indolequinone mechanism-based inhibitors of NAD(P)H:quinone oxidoreductase 1 (NQO1): NQO1 inhibition and growth inhibitory activity in human pancreatic MIA PaCa-2 cancer cells, Biochemistry 46 (2007) 5941–5950.
[66] R. Cone, S.K. Hasan, J.W. Lown, A.R. Morgan, The mechanism of the degradation of DNA by streptonigrin, Can. J. Biochem. 54 (1976) 219–223.
[67] H. Zhou, L. Huang, Y. Sun, B. Rigas, Nitric oxide-donating aspirin inhibits the growth of pancreatic cancer cells through redox-dependent signaling, Cancer Lett. 273 (2009) 292–299.
[68] R. Zhang, I. Humphreys, R.P. Sahu, Y. Shi, S.K. Srivastava, In vitro and in vivo induction of apoptosis by capsaicin in pancreatic cancer cells is mediated through ROS generation and mitochondrial death pathway, Apoptosis 13 (2008) 1465–1478.
[69] R. Zhang, S. Loganathan, I. Humphreys, S.K. Srivastava, Benzyl isothiocyanate-induced DNA damage causes G2/M cell cycle arrest and apoptosis in human pancreatic cancer cells, J. Nutr. 136 (2006) 2728–2734.
[70] B.N. Fahy, M. Schlieman, S. Virudachalam, R.J. Bold, AKT inhibition is associated with chemosensitisation in the pancreatic cancer cell line MIA-PaCa-2, Br. J. Cancer 89 (2003) 391–397.
[71] E. Cadenas, Antioxidant and prooxidant functions of DT-diaphorase in quinone metabolism, Biochem. Pharmacol. 49 (1995) 127–140.